ACS BIO & MED CHEM Au
AN OPEN ACCESS JOURNAL OF THE AMERICAN CHEMICAL SOCIETY

pubs.acs.org/biomedchemau

Article

Discovery of a New Chemoeffector for *Escherichia coli* Chemoreceptor Tsr and Identification of a Molecular Mechanism of Repellent Sensing

Xi Chen,[⊥] Shuangyu Bi,*[,⊥] Xiaomin Ma, Victor Sourjik, and Luhua Lai*

Cite This: *ACS Bio Med Chem Au* 2022, 2, 386–394

Read Online

ACCESS | Metrics & More | Article Recommendations | Supporting Information

ABSTRACT: Motile bacteria use chemotaxis to search for nutrients and escape from harmful chemicals. While the sensing mechanisms for chemical attractants are well established, the molecular details of chemorepellent detection are poorly understood. Here, by using combined computational and experimental approaches to screen potential chemoeffectors for the *Escherichia coli* chemoreceptor Tsr, we identified a specific chemorepellent, 1-aminocyclohexanecarboxylic acid (ACHC). Our study strongly suggests that ACHC directly binds to the periplasmic sensory domain of Tsr and competes with L-serine, the amino acid attractant of Tsr. We further characterized the binding features of L-serine, ACHC, and L-leucine (a natural repellent that binds Tsr) and found that Asn68 plays a key role in mediating chemotactic response. Mutating Asn68 to Ala inverted the response to L-leucine from a repellent to an attractant. Our study provides important insights into the molecular mechanisms of ligand sensing via bacterial chemoreceptors.

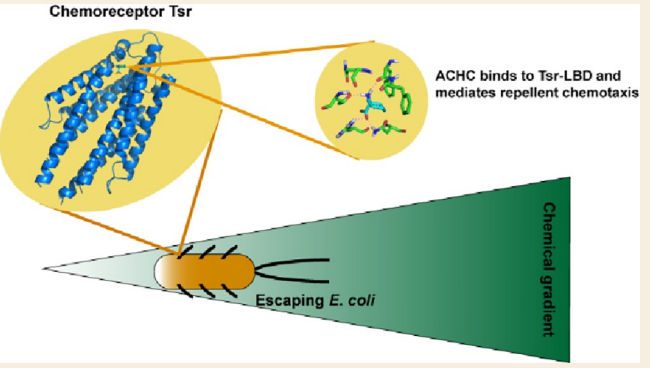

KEYWORDS: *chemotaxis, chemoreceptor, repellent, attractant, virtual screening, microfluidics*

INTRODUCTION

Many motile bacteria perform chemotaxis toward or away from spatial gradients of environmental stimuli to find physiologically favorable conditions.[1−3] Various extracellular signals are integrated by a robust chemotaxis network, in which the core of signal processing is a ternary complex formed by chemoreceptors, a histidine kinase CheA, and an adaptor CheW that controls the autophosphorylation activity of CheA. In *Escherichia coli*, positive chemotactic stimuli (attractants) inhibit CheA and promote a kinase-off state, whereas negative chemotactic stimuli (repellents) stimulate it and promote a kinase-on state. CheA subsequently donates the phosphoryl group to the response regulator CheY to form CheY-P, which elicits the clockwise rotation of the flagellar motor(s) and promotes transient tumbles. Dephosphorylation of CheY-P is mediated by the phosphatase CheZ. After the initial response, an adaptation system composed of a methyltransferase CheR and a methylesterase CheB adjusts the levels of receptor methylation and thereby the kinase activity.

The high-abundance chemoreceptors Tsr and Tar enable *E. coli* cells to sense multiple amino acids and several other stimuli using a variety of mechanisms.[4−6] Tsr mainly mediates attractant responses to serine, which also senses other amino acid attractants, including cysteine, asparagine, alanine, glycine, and quorum signaling molecule autoinducer 2 (AI-2).[7,8] Tsr further mediates repellent responses to several chemical compounds, including leucine, isoleucine, tryptophan, phenol, indole, and hormones as well as general physicochemical stimuli such as pH and osmolarity.[7,9−16] The periplasmic ligand-binding domain (LBD) of Tsr is known to bind amino acid attractants directly via its ligand-binding pocket[17] and to monitor the AI-2 concentration indirectly via the interaction with its respective periplasmic binding protein LsrB.[8] Although the sensing mechanisms of chemical attractants have been extensively studied, the detection mechanisms for repellent molecules remain elusive. They are likely to be sensed by perturbating different regions of the chemoreceptors, including not only the periplasmic[7] but also the cytoplasmic domains.[9] Although a previous study indicated that the LBD of Tsr contains the determinants to detect leucine,[7] the underlying sensing mechanisms remain unclear, and no other repellent molecules that bind directly to the LBDs of *E. coli* chemoreceptors have been characterized.

Received: November 7, 2021
Revised: March 3, 2022
Accepted: March 9, 2022
Published: March 18, 2022

https://doi.org/10.1021/acsbiomedchemau.1c00055
ACS Bio Med Chem Au 2022, 2, 386−394

Although the *E. coli* chemotaxis pathway is one of the most conserved and best-studied signaling systems in bacteria, many aspects of signal transduction through chemoreceptors remain unclear. Even for the conventional response to chemical attractants, elucidating the detailed mechanisms of signal transduction has been difficult.[4,5] The conformational changes of the LBD upon attractant binding have been best studied for the chemoreceptor Tar. The binding of its primary attractant aspartate is believed to elicit an asymmetric 1−2 Å inward displacement of the last α-helix (α4) of Tar that extends into the second transmembrane helix (TM2)[5,18] as well as the rotation of the two monomers within the receptor dimer.[19] Although Tsr-LBD forms a similar protein structure to Tar-LBD,[17] the details of the conformational changes promoted by ligand binding are less known. The crystal structures and molecular dynamics (MD) simulations of the unbound and attractant-bound Tsr suggest that the conformational changes in the α4 of the LBD are important for chemotactic signaling.[17,20] The conformational changes of the LBD tune the rigidity and helicity of the five-residue control cable,[21,22] which transmits signals to the HAMP domain of Tsr and further influences the dynamics of the methylation helix bundle, flexible bundle, and signaling tip.[23−25] However, the exact mechanism by which ligand binding to Tsr-LBD triggers these conformational changes remains unclear.

Attractant binding and methylation are thought to elicit opposing conformational changes in receptors that shift the CheA equilibrium between the kinase-on and kinase-off activity states. However, without an established directly binding repellent, the exact conformational changes promoted by negative chemotactic stimuli remain unclear. Although multiple mutations in different receptor regions are known to activate CheA kinase,[21,22,24,26−38] some of them could affect the sensitivity to attractant stimulation, while their sensitivity to repellent stimulation was not tested, thus failing to provide direct mechanistic insights into repellent signaling.

The discovery of novel chemoeffectors provides molecular probes to uncover receptor signaling mechanisms. Virtual screening, an approach that has been used extensively in the drug discovery process,[39] is a powerful tool for novel chemoeffector identification. We have previously used virtual screening and experimental approaches to search for compounds that bind to Tar-LBD from a large chemical library and discovered novel attractants and antagonists.[40] However, no repellent molecules that bind to Tar-LBD were found in that screening.

In the present study, by using an integrated *in silico*, *in vitro*, and *in vivo* approach, we identified 1-aminocyclohexanecarboxylic acid (ACHC) as a novel chemical repellent sensed by Tsr-LBD. We showed that ACHC binds directly to the same ligand-binding pocket as the amino acid attractant L-serine, and similar sensing mechanisms are used by Tsr in response to the amino acid repellent L-leucine. We further elucidated the molecular mechanisms by which bacterial receptors accommodate attractants and repellents at the same binding site to promote opposite responses, thereby providing critical insights into ligand recognition by chemoreceptors.

RESULTS

Virtual Screening for Potential Novel Tsr-Specific Chemoeffectors

We performed molecular docking-based virtual screening against the Tsr-LBD ligand-binding site. The crystal structures of the Tsr-LBD dimer bound to two L-serine molecules (holo structure, PDB ID: 3ATP) or without a ligand (apo structure, PDB ID: 2D4U) have been reported previously.[17] We used the apo structure (2D4U) with C36D mutation (see the Experimental Section) to perform virtual screening to identify potential chemoeffectors that might bind to Tsr-LBD. The possible ligand-binding pockets were searched on the protein surface of Tsr-LBD, and the serine binding pocket was identified as the best pocket for compound binding. We first carried out molecular docking of L-serine with Tsr-LBD using the AutoDock program,[41] and the docking score was −6.07 kcal mol^{-1}. Molecular docking screening from the Available Chemical Directory (Elsevier MDL; https://www.daylight.com/products/acd.html) was performed, and the candidate compounds were docked to the L-serine binding pocket around the residues R64, N68, and F151 to Q157. Due to the limited size of the pocket, compounds with molecular weights less than 300 Da (~150,000 compounds) were used in the docking study. The top 20,000 compounds with the lowest estimated binding free energies lower than −5.5 kcal mol^{-1} were selected. The compounds were then manually selected according to their structures and binding conformations in the pocket. Compounds that formed hydrogen bonds with the key residues in the pocket were prioritized, and 37 compounds were selected for further experimental studies (Table S1).

Discovery of a Novel Repellent that Functions through Tsr-LBD

We measured the responses of *E. coli* receptorless strain UU1250[42] expressing wild-type Tsr as the sole receptor and green fluorescent protein (GFP) to these 37 compounds using a modified microfluidic device reported previously[43] (see the Experimental Section and Figure S1). This device is suitable for both attractant and repellent detection from a compound library. *E. coli* cells were loaded into the sink pore of the device and allowed to swim into the observation channel. The compound solution was then loaded into the source pore and allowed to gradually diffuse through the agarose gel into the observation channel to form a concentration gradient. If the compound is an attractant, then bacterial cells sense the attractant gradient and move from the sink pore into the observation channel to accumulate toward the source, increasing the cell intensity in the observation channel. However, if the compound is a repellent, then cells sense the gradient and move out of the observation channel toward the sink pore, decreasing the cell intensity.

We used L-serine and L-leucine as positive controls for attractant and repellent responses, respectively. The GFP-labeled cells drifted up the L-serine gradient in the observation channel, and the number of cells accumulated in the observation channel increased over time (Figure S2). In contrast, cells exhibited a repellent response to L-leucine as the number of cells in the observation channel decreased (Figure 1). Among the 37 compounds, Tsr mediates a robust repellent response to an unnatural amino acid, 1-aminocyclohexanecarboxylic acid (ACHC, ACD number 78621; Figure 1a), with cells moving down the gradient of ACHC and thus out of the observation channel into the sink pore (Figure 1b,c). This

https://doi.org/10.1021/acsbiomedchemau.1c00055
ACS Bio Med Chem Au 2022, 2, 386−394

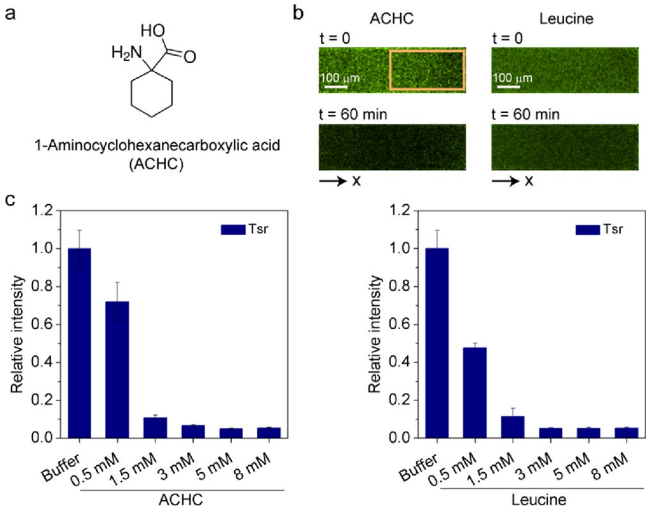

Figure 1. Microfluidic assay of the chemotactic response of the receptorless strain UU1250 expressing Tsr as the sole receptor to ACHC and L-leucine. (a) Chemical structure of ACHC. (b) Examples of cell distribution in the observation channel of the microfluidic device, acquired before the addition of ligands and 60 min after the addition of 8 mM ACHC or L-leucine at the source pore (scale bar, 100 μm). The x-component (black arrow) indicates the direction up the concentration gradient of ACHC or L-leucine. The response is characterized by measurements of the fluorescence intensity (cell density) in the analysis region (150 μm × 300 μm) of the observation channel indicated by a yellow rectangle. (c) Relative fluorescence intensity in the analysis region of the observation channel 60 min after the addition of indicated ligand concentrations at the source or without a ligand (buffer). The corresponding values of the fluorescence intensities in the analysis regions are normalized to the fluorescence intensity of cells in buffer. Error bars indicate the standard errors of three replicates.

repellent response was concentration-dependent and resembled the response to L-leucine, indicating that ACHC might be a novel Tsr-specific repellent.

To investigate whether the response to ACHC is mediated by Tsr-LBD, we measured the responses of cells expressing either the chemoreceptor Tar or the hybrid receptors that combine the sensory domain of Tsr with the signaling domain of Tar (Tsar)[10] or vice versa (Tasr) or the responses of the wild-type *E. coli* strain RP437[44] expressing all five *E. coli* chemoreceptors (Figure S3). We observed that the wild-type *E. coli* and the cells expressing Tsar showed robust repellent responses to ACHC. In contrast, the cells expressing Tar or Tasr did not show obvious responses at the tested concentrations, suggesting that ACHC works through Tsr-LBD.

We further investigated whether the Tsr response to L-leucine is mediated through a mechanism similar to that of ACHC. Indeed, Tsar-expressing and wild-type *E. coli* exhibited repellent responses to L-leucine (Figure 1b,c and Figure S3), whereas Tar-only and Tasr-only cells showed no response (Figure S3). These results are consistent with those of a previous study, suggesting that Tsr-LBD directly senses L-leucine.[7]

In Vivo Responses to ACHC Measured by FRET

We further characterized the signaling properties of Tsr in response to ACHC *in vivo* using a reporter assay based on fluorescence (Förster) resonance energy transfer (FRET).[45,46] Unlike the microfluidic assay that measures the swimming responses of bacteria to a given compound gradient, the FRET assay monitors the interaction between CheY fused to yellow fluorescent protein (CheY-YFP) and its phosphatase CheZ fused to cyan fluorescent protein (CheZ-CFP) upon the addition or removal of ambient concentrations of attractants or repellents. Because this interaction requires CheY phosphorylation by CheA, increased CheA activity results in a stronger FRET signal and therefore a higher ratio of YFP to CFP fluorescence. The Tsr receptor was expressed from a plasmid in the strain VS181,[46] which lacks all endogenous receptors and native *cheY* and *cheZ* genes but contains an intact receptor methylation system. FRET measurements further confirmed that Tsr mediates a repellent response to ACHC (Figure 2a,b)

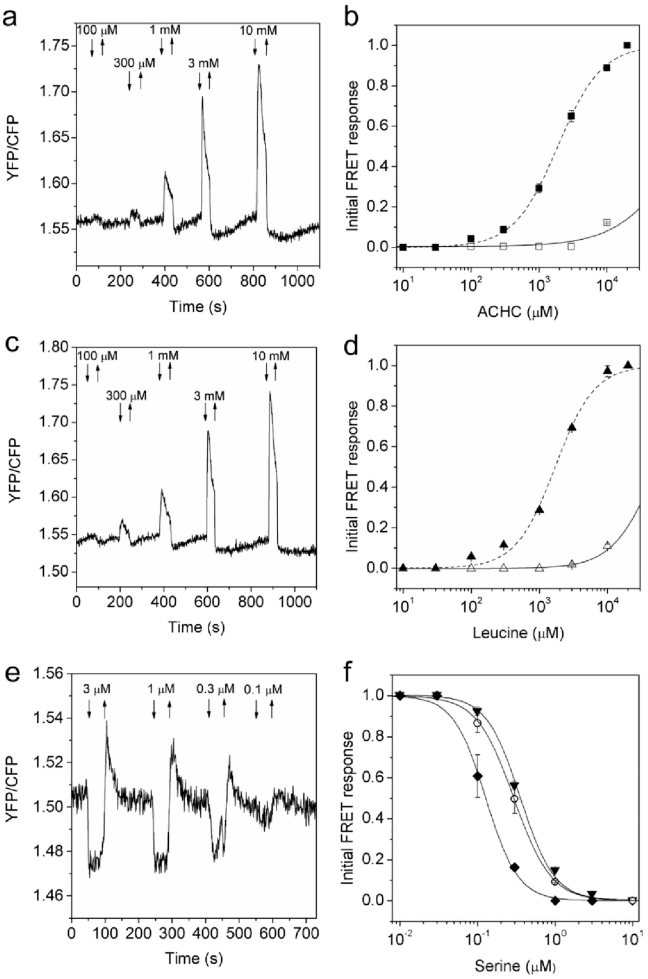

Figure 2. FRET measurements of response for *E. coli* cells expressing Tsr as the sole receptor to the indicated concentrations of ACHC and L-leucine. (a, c, e) FRET responses of buffer-adapted *E. coli* cells expressing Tsr as the sole receptor upon stepwise addition (down-arrow) and subsequent removal (up-arrow) of the indicated concentrations of ACHC (a), L-leucine (c), or L-serine (e). (b) Dose–response curve of Tsr to ACHC in buffer (closed squares) or in the presence of 200 μM L-serine (open squares). (d) Dose–response curve of Tsr to L-leucine in buffer (closed triangles) or in the presence of 200 μM L-serine (open triangles). (f) Dose–response curve of Tsr to L-serine in buffer (closed diamonds) or in the presence of 10 mM ACHC (open circles) or 10 mM L-leucine (closed triangles). In panels (b, d, f), error bars indicate the standard errors of three independent experiments; wherever invisible, error bars are smaller than the symbol size.

https://doi.org/10.1021/acsbiomedchemau.1c00055
ACS Bio Med Chem Au 2022, 2, 386–394

with an initial rapid increase in kinase activity (corresponding to the increase in the YFP/CFP ratio) upon stimulation. This is similar to the repellent response to L-leucine (Figure 2c,d) but opposite to the attractant response elicited by L-serine (Figure 2e,f). Ligand concentrations that elicited half-maximal response (EC_{50} values) were 1.9 ± 0.1, 1.7 ± 0.1, and 127 ± 6 nM for ACHC, L-leucine, and L-serine, respectively. Consistent with the microfluidic results, cells expressing Tsar and wild-type RP437 showed a repellent response to ACHC comparable to that mediated by Tsr, while Tar and Tasr mediated no or only a weak response (Figure S4), supporting our conclusion that the responses to ACHC are mediated by Tsr-LBD. These strains also showed similar responses to L-leucine, which is in accordance with a previous report.[7]

ACHC, L-Leucine, and L-Serine Apparently Bind to the Same Ligand-Binding Pocket of Tsr

To test whether ACHC or L-leucine competitively binds to the same binding pocket of L-serine, we adapted the Tsr receptor to a saturated level of one ambient ligand and measured the response to the other. The binding of ACHC, L-leucine, and L-serine to Tsr was apparently competitive for the same binding site because adaptation to 200 μM L-serine significantly inhibited the response to ACHC and L-leucine (Figure 2b,d). Meanwhile, adaptation to 10 mM ACHC and L-leucine raised the EC_{50} of the response to L-serine from 127 ± 6 to 294 ± 6 and 360 ± 14 nM, respectively (Figure 2f). It was previously shown that such mutual inhibition is only observed for the competitive binding of the two ligands, whereas saturation with a ligand that signals through the same chemoreceptor via a different mechanism has no effect on the response.[47]

In Vitro Binding of ACHC and L-Leucine to Tsr-LBD

We measured the *in vitro* binding affinities of ACHC and L-leucine with purified Tsr-LBD protein using microscale thermophoresis (MST). MST detects the direct movement of fluorescent molecules along temperature gradients in capillaries to quantify the interaction affinities. Binding of ligands typically changes the thermophoretic movement of the protein molecules, which can be used to derive dissociation constants (K_d) by sequentially scanning capillaries with varying ligand concentrations.[48] MST has been applied in studying weak binding systems and validated to give solid results.[49−51] The measured K_d of Tsr-LBD binding to L-serine was 207 μM (Figure S5), which is slightly larger than the previously reported K_d of 35.6 μM.[17] The repellent molecules ACHC and L-leucine bind to Tsr-LBD with K_d values of 10.6 ± 2.4 and 23.6 ± 6.8 mM, respectively (Figure 3). Competitive binding experiments were also performed to demonstrate that L-leucine or ACHC competes with L-serine for the same binding site. When the Tsr ligand-binding pocket was saturated with a high concentration of L-serine, L-leucine and ACHC could not bind to Tsr-LBD (Figure 3), suggesting that these repellents bind to the same ligand-binding pocket as L-serine in Tsr-LBD.

To further prove that ACHC and L-leucine bind to Tsr-LBD, we used differential scanning fluorimetry (DSF) to measure the changes in the relative stability of Tsr-LBD protein with or without these compounds. DSF is a technology used to measure protein stability by characterizing thermal unfolding, chemical denaturation, and aggregation.[52] Ligand binding might change protein stability, which can be represented by a change in melting temperature (Tm). We used ΔTm, which is the protein Tm value with compounds minus the Tm value without compounds to represent the increase in Tm. The free Tsr-LBD is relatively unstable, with a Tm of 39.65 °C. Upon incubation with different concentrations of L-serine, we observed that ΔTm increased with a concentration dependence of up to 7.89 ± 0.10 °C (Figure S6), consistent with the specific binding of L-serine to Tsr-LBD. Similarly, ΔTm increased by 0.65 ± 0.15 and 1.47 ± 0.10 °C when incubating Tsr with L-leucine and ACHC, respectively (Figure 4).

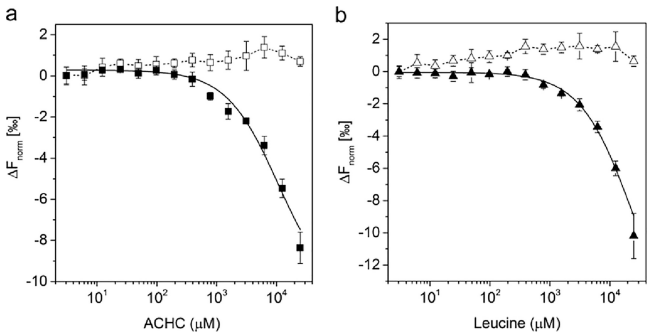

Figure 3. Microscale thermophoresis study of the interaction between fluorescently labeled Tsr-LBD and ACHC (a) or L-leucine (b). (a) The normalized thermophoresis signals are plotted against the ACHC concentrations in buffer (closed squares) or in the presence of 25 mM L-serine (open squares). (b) The normalized thermophoresis signals are plotted against the L-leucine concentrations in buffer (closed triangles) or in the presence of 25 mM L-serine (open triangles). Error bars indicate the standard errors of three independent experiments.

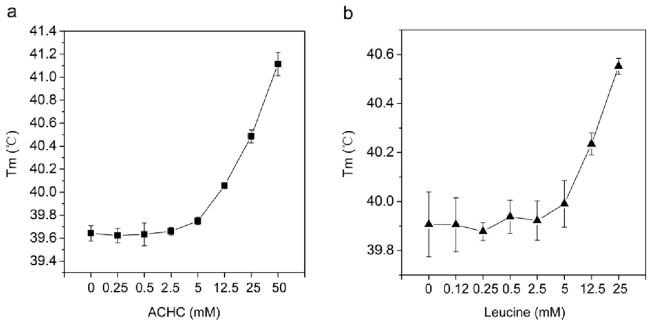

Figure 4. Melting temperature (Tm) for the Tsr periplasmic sensory domain at each concentration of ACHC (a) or L-leucine (b) determined by DSF. Error bars indicate the standard errors of three independent experiments.

Mutational Analysis of Ligand Interactions with Tsr-LBD

The ligand-binding pocket of Tsr-LBD contains residues R64, L67, N68, L136, L139, and F151-Q157 from one monomer and R69′ and I72′ from the other monomer. A previous study demonstrated that R64 and N68 are critical for L-serine sensing in Tsr.[17] The complex structure of the periplasmic domain of Tsr binding with L-serine shows that the side chains of R64 and N68 provide a cavity for the α-carboxyl group of L-serine, and the β-hydroxyl group of L-serine forms a hydrogen bond with the side chain of N68, which were also captured in our docking model (Figure 5a). Furthermore, a previous study showed that the mutation of N68 severely impairs serine binding, indicating its essential role in serine sensing.[17] Our molecular docking results showed that R64 and N68 are also important both for L-leucine and ACHC binding, with the side chains of R64 and N68 interacting with the α-carboxyl group of the compounds (Figure 5b,c). As N68 cannot form favorable interactions with

https://doi.org/10.1021/acsbiomedchemau.1c00055
ACS Bio Med Chem Au 2022, 2, 386−394

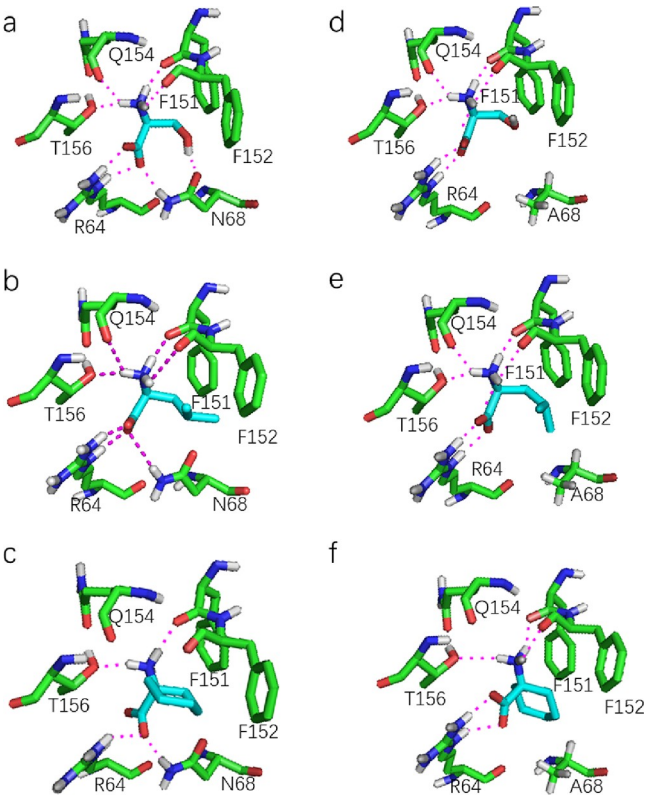

Figure 5. Binding site analysis using molecular docking. (a–c) Conformations of L-serine (a), L-leucine (b), and ACHC (c) binding to the wild-type Tsr-LBD. (d–f) Conformations of L-serine (d), L-leucine (e), and ACHC (f) binding to the mutant Tsr^{N68A}.

the hydrophobic side chains of L-leucine and ACHC, the orientations of these two compounds change with the hydrophobic side chains stretching toward the two hydrophobic residues (F151 and F152) in the upper-right position and avoiding the polar N68 side chain in the lower-right position of the binding site (Figure 5b,c). The loss of hydrogen-bond interactions and the reorientation of ligand side chains provide possible explanations that L-leucine and ACHC bind Tsr-LBD with weaker affinity than that of L-serine and act as repellents as we observed in the experiments.

To verify these key interactions, we constructed three Tsr mutants: Tsr^{R64A}, Tsr^{N68A}, and $Tsr^{R64AN68A}$ and measured their responses to all the three compounds using the microfluidic assay. As expected, Tsr^{R64A}, Tsr^{N68A}, and $Tsr^{R64AN68A}$ showed weaker attractant responses to L-serine (Figure S7) and weaker repellent responses to ACHC than the wild-type Tsr (Figure 6a), confirming that R64 and N68 play a key role in L-serine, ACHC binding, and sensing. In the case of L-leucine, Tsr^{R64A} and $Tsr^{R64AN68A}$ showed no response or much weaker responses at the tested concentrations, which was expected. However, it is interesting that Tsr^{N68A} mediated an attractant response to L-leucine (Figure 6b). This inverted response was verified by FRET measurements, where cells expressing Tsr^{N68A} as the sole receptor indeed exhibited a strong attractant response to L-leucine (Figure 6c). These results support that L-leucine interacts with residues R64 and N68 in the ligand-binding pocket of Tsr.

We further docked L-serine, L-leucine, and ACHC to the binding pocket of Tsr^{N68A} to explore the possible mechanisms of weakened or inverted responses to these compounds

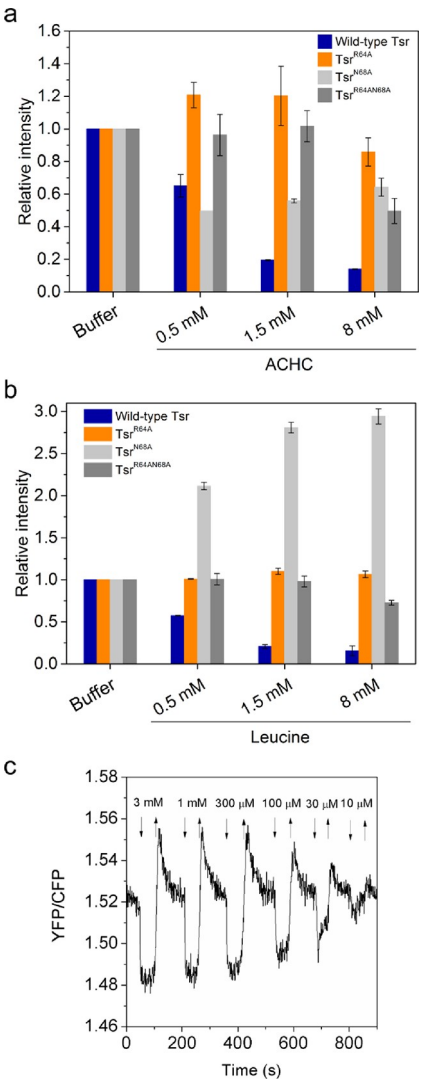

Figure 6. Measurements of the chemotactic response of *E. coli* cells expressing wild-type or mutant Tsr as a sole receptor to ACHC or L-leucine. (a, b) Microfluidic assay of the chemotactic responses of wild-type Tsr, Tsr^{R64A}, Tsr^{N68A}, and $Tsr^{R64AN68A}$ to indicated source concentrations of ACHC (a) or L-leucine (b). The response is characterized by measurements of the fluorescence intensity in the analysis region (150 μm × 300 μm) 60 min after ligand addition. The corresponding values of the fluorescence intensities in the analysis regions are normalized to the fluorescence intensity of cells in buffer. Error bars indicate the standard errors of three replicates. (c) FRET measurements for buffer-adapted *E. coli* cells expressing Tsr^{N68A} as the sole receptor stimulated with indicated concentrations of L-leucine.

(Figure 5d–f). The predicted binding energies for these ligands interacting with Tsr^{N68A} can be found in Table S2. Mutating N68 to A68 destroyed the hydrogen bonds between the side chain of N68 and the hydroxyl group of L-serine in the wild-type Tsr (Figure 5d), thereby weakening the binding affinity and leading to a weaker attractant response (Table S2 and Figure S7). In contrast, the binding conformation of L-leucine to Tsr^{N68A} was quite different from that of wild-type Tsr (Figure 5b,e) with its hydrophobic side chain moving down to form hydrophobic interactions with A68, which provide "attraction forces" similar to the hydrogen bonds formed between the side chain of L-serine and N68 in the wild-type Tsr. This likely explains why Tsr^{N68A} mediates an

https://doi.org/10.1021/acsbiomedchemau.1c00055
ACS Bio Med Chem Au 2022, 2, 386–394

inverted, attractant response to L-leucine. For ACHC, the hydrogen bonds formed between the side chain of N68 and the α-carboxyl group of ACHC were lost in Tsr^{N68A}, explaining a weaker binding affinity and chemotactic response mediated by this receptor (Table S2 and Figure S7). Unlike L-leucine, ACHC still triggers a weak repellent response of Tsr^{N68A}, possibly because its hextomic ring still forms a favorable interaction with Phe151/Phe152, and the spatial restraint of the hexatomic ring weakens the hydrophobic interaction with A68, thus losing the attraction forces similar to the hydrophobic interaction between the side chain of L-leucine and A68.

DISCUSSION

E. coli cells sense certain repellent molecules, including fatty acids, aliphatic alcohols, amino acids, indole, aromatic compounds, inorganic ions, and mercaptans.[53] Most of these repellents are toxic compounds that are harmful to the cells.[7,53] Although a few repellents are specific for a particular chemoreceptor, neither the sensory modes nor the mechanisms of signaling has been established. Previous reports indicated that some non-canonical repellent stimuli (the indirect-binding repellents that act in other ways) seem to act downstream of the ligand-binding domains of chemoreceptors,[6,10] thus likely shifting the dynamic equilibrium of chemoreceptors from the kinase-off toward the kinase-on state, which is in a very different way from canonical ligands (ligands bind to the ligand-binding pocket of the chemoreceptor) via the direct-binding mechanism. However, the molecular mechanism of signaling by these non-canonical stimuli has not been elucidated. Therefore, the interpretation of the observed repellent response remained unclear for over three decades since their first observation. Discovering more specific repellents and understanding their molecular mechanism will provide useful information about receptor signaling in chemotaxis.

Here, we used *in silico* screening and subsequent experimental validations to identify a novel repellent ACHC that binds directly to the ligand-binding pocket of the *E. coli* chemoreceptor Tsr. Observations from different experimental approaches strongly suggest that the response to ACHC and to another known repellent, L-leucine, is mediated by their direct binding to the same site on Tsr-LBD as the canonical attractant L-serine. To our knowledge, this is the first time that direct-binding repellents as canonical ligands are reported for *E. coli*, providing a great opportunity to understand the repellent sensing mechanism. Our study confirmed the previous report that Tsr-LBD contains the determinant for L-leucine sensing and enabled us to characterize the detailed interactions with L-leucine and the new repellent compound found in this study. Given that the repellent response to L-leucine might be used by *E. coli* to avoid toxic levels of this non-catabolized amino acid,[7] it would be interesting to explore the physiological relevance of such competitive binding for L-leucine and L-serine detection.

We used molecular docking and mutation experiments to identify key interacting residues in Tsr for L-serine, L-leucine, and ACHC binding. We demonstrated that both attractants and repellents bind to the pocket formed by residues R64, N68, F151, F152, Q154, and T156. We found that Tsr-N68 plays a key role in eliciting positive chemotactic signals, and F151/F152 are important in eliciting negative chemotactic signals. The predicted binding modes of attractant L-serine, repellent ACHC, and L-leucine indicate that the key difference between the two classes of ligands is whether they form favorable interactions with N68 or F151/F152. The single mutation of N68A reversing the response to L-leucine from a repellent to an attractant also suggests the important function of N68 or the mutating residue at this position in mediating attractant signaling. Our results suggest that the interaction of the ligand with residue 68 forms an attraction force to elicit attractant responses as the hydrogen bond formed between the hydroxyl group of L-serine and N68 in the wild-type Tsr or the hydrophobic interaction formed between the side chain of L-leucine and A68 in Tsr^{N68A}. This provides an excellent system for further understanding the mechanism of ligand sensing by Tsr. Further determination of the complex structures, molecular dynamics simulations, and dynamic interaction analysis can be performed in future studies.

Although thousands of chemoreceptor genes have been identified in bacteria, there are only a small number of receptors for which ligand specificity has been established. Functional annotation of chemoreceptors remains a challenging task. One problem is that the sequential and structural conservation of receptor LBDs is typically low so that they can accommodate different types of ligands.[54] Even receptors with the same class of LBDs, such as the four-helix bundle (4HB) domains, appear to have an exceptionally broad range of specificity.[55] Moreover, similarities in ligand profiles are typically not reflected in the sequence or structural similarities of LBDs. Therefore, ligand discovery requires a combination of computational and experimental approaches. Recently, several experimental approaches have been developed that enable the systematic characterization of chemosensory specificities of bacterial chemoreceptors. These include the construction of hybrid receptors and signaling kinases that can be assayed for their chemosensing in a model system[56−58] as well as purification and characterization of ligand-binding domains.[59,60] Moreover, bioinformatic analysis of chemoreceptors has been applied to classify sensory domains and to predict their specificities.[61] Here, we show that ligand prediction by virtual screening and molecular docking is a powerful tool to discover candidate chemoeffectors of bacterial chemoreceptors, with the potential to identify novel attractants and antagonists as well as novel repellents. As chemotaxis is an important virulence factor for pathogens, repelling pathogenic bacteria might provide a promising therapeutic strategy to prevent disease. Identification of repellents that directly interact with chemoreceptors may provide useful clues for the rational design of repellents to prevent the chemoattraction of pathogenic bacteria.

The observed inverted chemotactic response of Tsr^{N68A} to L-leucine demonstrates the surprising plasticity of a bacterial chemoreceptor, enabling it to accommodate attractants and repellents in the same ligand-binding site. Finally, the inversion of the chemotactic signal by a single mutation in the receptor might have a potential application in controlling the response sign of the target compound for chemoreceptor-based biosensor designs.

EXPERIMENTAL SECTION

Virtual Screening

AutoDock 4.0.1[41] was used to perform molecular docking to screen potential chemoeffectors that might bind to Tsr-LBD. The configuration of Tsr-LBD used for the AutoDock screening was based on the apo Tsr-LBD structure (PDB ID: 2D4U) with a C36D

https://doi.org/10.1021/acsbiomedchemau.1c00055
ACS Bio Med Chem Au 2022, 2, 386−394

mutation and has been reported in our previous study with a detailed description of the structure preparation.[19] We then searched all possible ligand-binding pockets on the protein surface of Tsr-LBD, and the serine-binding pocket was identified as the best pocket for compound binding. The amino acids that belong to the serine-binding pocket were defined precisely and were used to do virtual screening by AutoDock. A docking box was constructed around the serine-binding pocket. Each compound was then placed in a box. The AutoDock program can simulate the possible conformations of this compound in the box, compute the binding energy of these conformations with a generic algorithm, and finally output the minimum binding energy and the best conformation. Molecular docking screening from the Available Chemicals Directory was performed, and the candidate compounds were docked to the serine-binding pocket. The top 20,000 compounds with the lowest estimated binding free energies lower than −5.5 kcal mol^{-1} and the molecular weights less than 300 Da were selected at first. Compounds were then manually selected with the following criteria: (i) being among the top 3500 compounds ranking by binding energies; (ii) with NH_3, NO_3, or OH groups that can form hydrogen bonds with Tsr-LBD; and (iii) being able to be purchased from chemical compound agencies. Finally, 37 compounds were selected for further experimental studies (Table S1).

Strains and Plasmids

The *E. coli* strains and plasmids used in this study are listed in Table S3. For FRET measurements, wild-type RP437 and the receptorless *cheY cheZ* strain VS181 [Δ(*cheYcheZ*)Δ*aer*Δ*tsr*Δ(*tar-tap*)Δ*trg*][46] were transformed with the plasmid pVS88 expressing the FRET pair CheY-YFP/CheZ-CFP. The receptorless strain UU1250 [Δ*aer*Δ*tsr*Δ(*tar-tap*)Δ*trg*][42] was used for the microfluidic assay. *E. coli* strain BL21(DE3) was used to express Tsr-LBD.

Molecular Cloning and Mutagenesis

pPA114 is a salicylate-inducible plasmid that encodes the full-length Tsr. The GFP gene fragment was amplified and digested with the restriction enzymes AvaI and BamHI. The pPA114 plasmid was dissected with AvaI and BamHI, and then, the GFP fragment was ligated into pPA114 to generate the plasmid pXC1 (Table S3). The plasmids pXC2 to pXC4 are mutants of pXC1 generated by a Q5 site-directed mutagenesis kit (New England BioLabs, Ipswich, MA, USA) using the plasmid pXC1 as the template. The plasmid pXC5 is a Tsr-N68A mutant generated using pPA114 as the template. The plasmid pXC6 was constructed by cloning Tsr residues 30−190 into pET28a with an N-terminal 6× His-tag, which is used for Tsr-LBD protein expression.

Microfluidic Assay

E. coli cells expressing receptor(s) of interest and GFP were grown at 34 °C in tryptone broth (TB; 1% tryptone and 0.5% NaCl) supplemented with appropriate concentrations of antibiotics (100 μg mL^{-1} ampicillin; 17 μg mL^{-1} chloramphenicol) and inducers (Table S3) until the OD_{600} reached 0.6. Cells were harvested by centrifugation and washed twice with tethering buffer (10 mM KH_2PO_4/K_2HPO_4, 0.1 mM EDTA, 1 μM methionine, and 10 mM sodium lactate; pH 7.0). The responses of *E. coli* cells to the concentration gradient of the compounds were measured using a microfluidic device described previously[43] (Figure S1). Briefly, 4% agarose was added to the source-side pore to flow into the agarose gel channel and seal the interface with the observation channel. *E. coli* cells were added to the sink pore and allowed to diffuse into the observation channel for 1 h. The compound solution was added to the source pore and allowed to gradually diffuse through the agarose channel into the observation channel. Cell fluorescence in the observation channel was measured using a Nikon Ti-E inverted fluorescence microscope (Nikon Instruments, Tokyo, Japan) with a 20× objective lens and Lumencor SOLA-SEII equipped with an Andor Zyla sCMOS camera. Cellular response was characterized by the fluorescence intensity (cell density) in the analysis region (150 μm × 300 μm) of the observation channel. Afterward, the data were analyzed using the ImageJ software.

FRET Measurements

E. coli cells with the plasmid encoding the FRET pair CheY-YFP/CheZ-CFP were grown at 34 °C and 275 rpm in TB supplemented with antibiotics and inducers until OD_{600} reached 0.6. The cells were harvested and washed twice with tethering buffer. FRET measurements were performed using an upright fluorescence microscope (Zeiss Axio Imager.Z1) as described previously.[10] Cells were attached to a polylysine-coated coverslip and placed in a flow chamber. Under a constant flow (0.5 mL min^{-1}), cells were stimulated with compounds of interest. Fluorescence signals were continuously recorded in the cyan and yellow channels using photon counters with a 1.0 s integration time. Data were plotted and analyzed as previously described.[10] For the repellent response, $Y = A \times L^H/(L^H + K^H)$, whereas for the attractant response, $Y = A \times (1 - L^H/(L^H + K^H))$. In the model, Y is the initial FRET response, L is the concentration of the ligand, A is the amplitude, H is the Hill coefficient, and K is the EC_{50}.

Protein Expression and Purification of the Tsr Periplasmic Domain

The plasmid pXC6 was transferred into *E. coli* BL21(DE3) cells to express the target proteins. An overnight culture of cells with the plasmids was diluted 1:100 with a Luria Bertani (LB) medium supplemented with 30 μg mL^{-1} kanamycin and grown at 37 °C and 340 rpm. When the OD_{600} value reached 0.6−0.8, 1 mM isopropyl β-D-thiogalactopyranoside (IPTG) was added to induce the expression of the target proteins. The induction time for expression was 6 h at 28 °C. The cells were then lysed by sonication in a sonication buffer (50 mM Tris−HCl, pH 8.0, 200 mM NaCl, and 2 mM PMSF). Cell debris was pelleted by centrifugation, and the supernatant was applied to a 5 mL HisTrap HP column (GE Healthcare) equilibrated with buffer A (50 mM Tris−HCl, pH 8.0, 200 mM NaCl, and 10 mM iminazole). A linear gradient of buffer B (50 mM Tris−HCl, pH 8.0, 200 mM NaCl, and 500 mM iminazole) was applied to elute the target proteins. The peak fraction containing target proteins from the HisTrap HP column was applied to a Sephacryl S-200 HR 16/60 column (GE Healthcare) equilibrated with buffer C (50 mM Tris−HCl, pH 8.0, and 200 mM NaCl). The proteins were eluted using the same buffer.

Microscale Thermophoresis (MST)

Thermophoresis is the directed movement of molecules within a temperature gradient. It depends on thermophoretic properties such as charge, size, and the hydration shell of migrating molecules.[48] MST is a technique that detects the thermophoresis of fluorescent protein molecules in capillaries to quantify binding affinities. The binding of compounds typically changes the properties of the protein, resulting in changes in the thermophoretic movement of the protein molecule, which can be used to derive dissociation constants (K_d). Purified Tsr-LBD with the His-tag was labeled with a His-tag dye (MO-L008 Monolith His-Tag labeling kit RED-tris-NTA, NanoTemper Technologies) at a final concentration of 0.05 mM. The compounds were diluted in a series of concentrations in HEPES buffer and mixed 1:1 with the protein. Afterward, the mixtures were loaded into the capillaries (MO-K002 Monolith NT.115 standard treated capillaries, NanoTemper Technologies). The MST measurement was performed using a Monolith NT.115 (NanoTemper Technologies) with 60% excitation power and 20% MST power. Normalized MST time traces record the thermophoretic movement of the labeled protein by the fluorescence changes in different concentrations of compounds and fit the dose−response curves with the "temperature jump and thermophoresis" mode. Data analysis was performed using the MO.Affinity Analysis v2.1.3 (NanoTemper Technologies) and Origin software.

Differential Scanning Fluorimetry (DSF)

The Tsr-LBD protein was prepared at a final concentration of 0.4 mg mL^{-1} in HEPES buffer (100 mM HEPES, 200 mM NaCl; pH 8.0). The compounds were diluted in a series of concentrations in HEPES buffer and mixed 1:1 with the protein. Protein samples were loaded

https://doi.org/10.1021/acsbiomedchemau.1c00055
ACS Bio Med Chem Au 2022, 2, 386−394

into standard Prometheus NT.48 capillaries. DSF measurements were performed using a Prometheus NT.48 (NanoTemper Technologies) over a temperature range of 20−90 °C with a ramp rate of 1 °C min^{-1}. The Tm of the Tsr protein with or without different concentrations of compounds was measured, and the ΔTm was calculated.

■ ASSOCIATED CONTENT

Supporting Information

The Supporting Information is available free of charge at https://pubs.acs.org/doi/10.1021/acsbiomedchemau.1c00055.

Microfluidic device used to measure the chemotactic responses of *E. coli*, the microfluidic assay of the chemotactic response of the receptorless *E. coli* cells expressing Tsr as the sole receptor to L-serine, the microfluidic assay of the chemotactic response of the mutant strains or the wild-type *E. coli* strain RP437 to ACHC and L-leucine, FRET responses of *E. coli* cells to ACHC and L-leucine, microscale thermophoresis study of the interaction between fluorescently labeled Tsr-LBD and L-serine, the melting temperature (Tm) for the Tsr periplasmic sensory domain at each concentration of L-serine determined by DSF, the microfluidic assay of the chemotactic responses of wild-type Tsr and the mutants to the indicated source concentrations of L-serine, compounds used in the experimental study and their predicted binding free energies, and the predicted binding free energies of wild-type Tsr-LBD and Tsr^{N68A} with the ligands, plasmids, and *E. coli* strains used in this study (PDF)

■ AUTHOR INFORMATION

Corresponding Authors

Shuangyu Bi − *Max Planck Institute for Terrestrial Microbiology & LOEWE Center for Synthetic Microbiology (SYNMIKRO), Marburg 35043, Germany; State Key Laboratory of Microbial Technology, Shandong University, Qingdao 266237, China*; Email: shuangyubi@sdu.edu.cn

Luhua Lai − *BNLMS, Peking-Tsinghua Center for Life Sciences at College of Chemistry and Molecular Engineering and Center for Quantitative Biology, Academy of Advanced Interdisciplinary Studies, Peking University, Beijing 100871, China*; orcid.org/0000-0002-8343-7587; Email: lhlai@pku.edu.cn

Authors

Xi Chen − *BNLMS, Peking-Tsinghua Center for Life Sciences at College of Chemistry and Molecular Engineering and Center for Quantitative Biology, Academy of Advanced Interdisciplinary Studies, Peking University, Beijing 100871, China*

Xiaomin Ma − *BNLMS, Peking-Tsinghua Center for Life Sciences at College of Chemistry and Molecular Engineering and Center for Quantitative Biology, Academy of Advanced Interdisciplinary Studies, Peking University, Beijing 100871, China*

Victor Sourjik − *Max Planck Institute for Terrestrial Microbiology & LOEWE Center for Synthetic Microbiology (SYNMIKRO), Marburg 35043, Germany*

Complete contact information is available at: https://pubs.acs.org/10.1021/acsbiomedchemau.1c00055

Author Contributions

⊥X.C. and S.B. contributed equally to this work; L.L. conceived and designed the research; X.C., S.B., X.M., and V.S. performed the research and analyzed the data; and X.C., S.B., V.S., and L.L. wrote the paper.

Notes

The authors declare no competing financial interest.

■ ACKNOWLEDGMENTS

This work was supported in part by the National Natural Science Foundation of China (21633001 to L.L. and 32070029 to S.B.) and by the Max Planck Society. We thank Prof. Chunxiong Luo and Prof. Qi Ouyang (Peking University) for the help of microfluidics experiments and Dr. Wei Yang (Peking University) for the help of computational work.

■ REFERENCES

(1) Colin, R.; Sourjik, V. Emergent properties of bacterial chemotaxis pathway. *Curr. Opin. Microbiol.* **2017**, *39*, 24−33.

(2) Porter, S. L.; Wadhams, G. H.; Armitage, J. P. Signal processing in complex chemotaxis pathways. *Nat. Rev. Microbiol.* **2011**, *9*, 153−165.

(3) Matilla, M. A.; Krell, T. Chemoreceptor-based signal sensing. *Curr. Opin. Biotechnol.* **2017**, *45*, 8−14.

(4) Bi, S.; Sourjik, V. Stimulus sensing and signal processing in bacterial chemotaxis. *Curr. Opin. Microbiol.* **2018**, *45*, 22−29.

(5) Parkinson, J. S.; Hazelbauer, G. L.; Falke, J. J. Signaling and sensory adaptation in *Escherichia coli* chemoreceptors: 2015 update. *Trends Microbiol.* **2015**, *23*, 257−266.

(6) Bi, S.; Jin, F.; Sourjik, V. Inverted signaling by bacterial chemotaxis receptors. *Nat. Commun.* **2018**, *9*, 2927.

(7) Yang, Y.; et al. Relation between chemotaxis and consumption of amino acids in bacteria. *Mol. Microbiol.* **2015**, *96*, 1272−1282.

(8) Hegde, M.; et al. Chemotaxis to the quorum-sensing signal AI-2 requires the Tsr chemoreceptor and the periplasmic LsrB AI-2-binding protein. *J. Bacteriol.* **2011**, *193*, 768−773.

(9) Pham, H. T.; Parkinson, J. S. Phenol sensing by *Escherichia coli* chemoreceptors: a nonclassical mechanism. *J. Bacteriol.* **2011**, *193*, 6597−6604.

(10) Yang, Y.; Sourjik, V. Opposite responses by different chemoreceptors set a tunable preference point in *Escherichia coli* pH taxis. *Mol. Microbiol.* **2012**, *86*, 1482−1489.

(11) Vaknin, A.; Berg, H. C. Osmotic stress mechanically perturbs chemoreceptors in *Escherichia coli*. *Proc. Natl. Acad. Sci. U. S. A.* **2006**, *103*, 592−596.

(12) Mao, H.; Cremer, P. S.; Manson, M. D. A sensitive, versatile microfluidic assay for bacterial chemotaxis. *Proc. Natl. Acad. Sci. U. S. A.* **2003**, *100*, 5449−5454.

(13) Lopes, J. G.; Sourjik, V. Chemotaxis of *Escherichia coli* to major hormones and polyamines present in human gut. *ISME J.* **2018**, *12*, 2736−2747.

(14) Pasupuleti, S.; et al. Chemotaxis of *Escherichia coli* to norepinephrine (NE) requires conversion of NE to 3,4-dihydroxymandelic acid. *J. Bacteriol.* **2014**, *196*, 3992−4000.

(15) Yang, J.; et al. Biphasic chemotaxis of *Escherichia coli* to the microbiota metabolite indole. *Proc. Natl. Acad. Sci. U. S. A.* **2020**, *117*, 6114−6120.

(16) Paulick, A.; et al. Mechanism of bidirectional thermotaxis in *Escherichia coli*. *Elife* **2017**, *6*, No. e26607.

(17) Tajima, H.; et al. Ligand specificity determined by differentially arranged common ligand-binding residues in bacterial amino acid chemoreceptors Tsr and Tar. *J. Biol. Chem.* **2011**, *286*, 42200−42210.

(18) Falke, J. J.; Hazelbauer, G. L. Transmembrane signaling in bacterial chemoreceptors. *Trends Biochem. Sci.* **2001**, *26*, 257−265.

(19) Yu, D.; Ma, X.; Tu, Y.; Lai, L. Both piston-like and rotational motions are present in bacterial chemoreceptor signaling. *Sci. Rep.* **2015**, *5*, 8640.
(20) Orr, A. A.; et al. Molecular mechanism for attractant signaling to DHMA by *E.coli* Tsr. *Biophys. J.* **2020**, *118*, 492−504.
(21) Ames, P.; Hunter, S.; Parkinson, J. S. Evidence for a helix-clutch mechanism of transmembrane signaling in a bacterial chemoreceptor. *J. Mol. Biol.* **2016**, *428*, 3776−3788.
(22) Kitanovic, S.; Ames, P.; Parkinson, J. S. A trigger residue for transmembrane signaling in the *Escherichia coli* serine chemoreceptor. *J. Bacteriol.* **2015**, *197*, 2568−2579.
(23) Parkinson, J. S. Signaling mechanisms of HAMP domains in chemoreceptors and sensor kinases. *Annu. Rev. Microbiol.* **2010**, *64*, 101−122.
(24) Zhou, Q.; Ames, P.; Parkinson, J. S. Mutational analyses of HAMP helices suggest a dynamic bundle model of input-output signalling in chemoreceptors. *Mol. Microbiol.* **2009**, *73*, 801−814.
(25) Samanta, D.; Borbat, P. P.; Dzikovski, B.; Freed, J. H.; Crane, B. R. Bacterial chemoreceptor dynamics correlate with activity state and are coupled over long distances. *Proc. Natl. Acad. Sci. U. S. A.* **2015**, *112*, 2455−2460.
(26) Lai, R. Z.; Parkinson, J. S. Functional suppression of HAMP domain signaling defects in the *E.coli* serine chemoreceptor. *J. Mol. Biol.* **2014**, *426*, 3642−3655.
(27) Ames, P.; Zhou, Q.; Parkinson, J. S. HAMP domain structural determinants for signaling and sensory adaptation in Tsr, the *Escherichia coli* serine chemoreceptor. *Mol. Microbiol.* **2014**, *91*, 875−886.
(28) Ortega, D. R.; et al. A phenylalanine rotameric switch for signal-state control in bacterial chemoreceptors. *Nat. Commun.* **2013**, *4*, 2881.
(29) Adase, C. A.; Draheim, R. R.; Rueda, G.; Desai, R.; Manson, M. D. Residues at the cytoplasmic end of transmembrane helix 2 determine the signal output of the TarEc chemoreceptor. *Biochemistry* **2013**, *52*, 2729−2738.
(30) Adase, C. A.; Draheim, R. R.; Manson, M. D. The residue composition of the aromatic anchor of the second transmembrane helix determines the signaling properties of the aspartate/maltose chemoreceptor Tar of *Escherichia coli*. *Biochemistry* **2012**, *51*, 1925−1932.
(31) Wright, G. A.; Crowder, R. L.; Draheim, R. R.; Manson, M. D. Mutational analysis of the transmembrane helix 2-HAMP domain connection in the *Escherichia coli* aspartate chemoreceptor tar. *J. Bacteriol.* **2011**, *193*, 82−90.
(32) Kitanovic, S.; Ames, P.; Parkinson, J. S. Mutational analysis of the control cable that mediates transmembrane signaling in the *Escherichia coli* serine chemoreceptor. *J. Bacteriol.* **2011**, *193*, 5062−5072.
(33) Mowery, P.; Ostler, J. B.; Parkinson, J. S. Different signaling roles of two conserved residues in the cytoplasmic hairpin tip of Tsr, the *Escherichia coli* serine chemoreceptor. *J. Bacteriol.* **2008**, *190*, 8065−8074.
(34) Ames, P.; Zhou, Q.; Parkinson, J. S. Mutational analysis of the connector segment in the HAMP domain of Tsr, the *Escherichia coli* serine chemoreceptor. *J. Bacteriol.* **2008**, *190*, 6676−6685.
(35) Draheim, R. R.; Bormans, A. F.; Lai, R. Z.; Manson, M. D. Tuning a bacterial chemoreceptor with protein-membrane interactions. *Biochemistry* **2006**, *45*, 14655−14664.
(36) Draheim, R. R.; Bormans, A. F.; Lai, R. Z.; Manson, M. D. Tryptophan residues flanking the second transmembrane helix (TM2) set the signaling state of the Tar chemoreceptor. *Biochemistry* **2005**, *44*, 1268−1277.
(37) Baumgartner, J. W.; Hazelbauer, G. L. Mutational analysis of a transmembrane segment in a bacterial chemoreceptor. *J. Bacteriol.* **1996**, *178*, 4651−4660.
(38) Gao, Q.; Cheng, A.; Parkinson, J. S. Conformational shifts in a chemoreceptor helical hairpin control kinase signaling in *Escherichia coli*. *Proc. Natl. Acad. Sci. U. S. A.* **2019**, *116*, 15651−15660.
(39) Rester, U. From virtuality to reality - virtual screening in lead discovery and lead optimization: a medicinal chemistry perspective. *Curr. Opin. Drug Discovery Dev.* **2008**, *11*, 559−568.
(40) Bi, S.; et al. Discovery of novel chemoeffectors and rational design of *Escherichia coli* chemoreceptor specificity. *Proc. Natl. Acad. Sci. U. S. A.* **2013**, *110*, 16814−16819.
(41) Huey, R.; Morris, G. M.; Olson, A. J.; Goodsell, D. S. A semiempirical free energy force field with charge-based desolvation. *J. Comput. Chem.* **2007**, *28*, 1145−1152.
(42) Ames, P.; Studdert, C. A.; Reiser, R. H.; Parkinson, J. S. Collaborative signaling by mixed chemoreceptor teams in *Escherichia coli*. *Proc. Natl. Acad. Sci. U. S. A.* **2002**, *99*, 7060−7065.
(43) Si, G.; Yang, W.; Bi, S.; Luo, C.; Ouyang, Q. A parallel diffusion-based microfluidic device for bacterial chemotaxis analysis. *Lab Chip* **2012**, *12*, 1389−1394.
(44) Parkinson, J. S.; Houts, S. E. Isolation and behavior of *Escherichia coli* deletion mutants lacking chemotaxis functions. *J. Bacteriol.* **1982**, *151*, 106−113.
(45) Sourjik, V.; Berg, H. C. Receptor sensitivity in bacterial chemotaxis. *Proc. Natl. Acad. Sci. U. S. A.* **2002**, *99*, 123−127.
(46) Sourjik, V.; Berg, H. C. Functional interactions between receptors in bacterial chemotaxis. *Nature* **2004**, *428*, 437−441.
(47) Neumann, S.; Hansen, C. H.; Wingreen, N. S.; Sourjik, V. Differences in signalling by directly and indirectly binding ligands in bacterial chemotaxis. *EMBO J.* **2010**, *29*, 3484−3495.
(48) Linke, P.; et al. An automated microscale thermophoresis screening approach for fragment-based lead discovery. *J. Biomol. Screening* **2016**, *21*, 414−421.
(49) Xiong, X.; et al. Receptor binding by a ferret-transmissible H5 avian influenza virus. *Nature* **2013**, *497*, 392−396.
(50) Westermaier, Y.; Veurink, M.; Riis-Johannessen, T.; Guinchard, S.; Gurny, R.; Scapozza, L. Identification of aggregation breakers for bevacizumab (Avastin) self-association through similarity searching and interaction studies. *Eur. J. Pharm. Biopharm.* **2013**, *85*, 773−780.
(51) Gao, M.; et al. Ca^{2+} sensor-mediated ROS scavenging suppresses rice immunity and is exploited by a fungal effector. *Cell* **2021**, *184*, 5391−5404.e17.
(52) Alexander, C. G.; et al. Novel microscale approaches for easy, rapid determination of protein stability in academic and commercial settings. *Biochim. Biophys. Acta* **2014**, *1844*, 2241−2250.
(53) Tso, W. W.; Adler, J. Negative chemotaxis in *Escherichia coli*. *J. Bacteriol.* **1974**, *118*, 560−576.
(54) Lacal, J.; García-Fontana, C.; Muñoz-Martínez, F.; Ramos, J. L.; Krell, T. Sensing of environmental signals: classification of chemoreceptors according to the size of their ligand binding regions. *Environ. Microbiol.* **2010**, *12*, 2873−2884.
(55) Gavira, J. A.; Matilla, M. A.; Fernández, M.; Krell, T. The structural basis for signal promiscuity in a bacterial chemoreceptor. *FEBS J.* **2021**, *288*, 2294−2310.
(56) Bi, S.; Pollard, A. M.; Yang, Y.; Jin, F.; Sourjik, V. Engineering hybrid chemotaxis receptors in bacteria. *ACS Synth. Biol.* **2016**, *5*, 989−1001.
(57) Lehning, C. E.; Heidelberger, J. B.; Reinhard, J.; Nørholm, M. H. H.; Draheim, R. R. A modular high-throughput *in vivo* screening platform based on chimeric bacterial receptors. *ACS Synth. Biol.* **2017**, *6*, 1315−1326.
(58) Luu, R. A.; et al. Hybrid two-component sensors for identification of bacterial chemoreceptor function. *Appl. Environ. Microbiol.* **2019**, *85*, No. e01626-19.
(59) Krell, T. Tackling the bottleneck in bacterial signal transduction research: high-throughput identification of signal molecules. *Mol. Microbiol.* **2015**, *96*, 685−688.
(60) Corral-Lugo, A.; et al. High-affinity chemotaxis to histamine mediated by the TlpQ chemoreceptor of the human pathogen *Pseudomonas aeruginosa*. *MBio* **2018**, *9*, No. e01894-18.
(61) Ortega, D. R.; et al. Assigning chemoreceptors to chemosensory pathways in *Pseudomonas aeruginosa*. *Proc. Natl. Acad. Sci. U. S. A.* **2017**, *114*, 12809−12814.

https://doi.org/10.1021/acsbiomedchemau.1c00055
ACS Bio Med Chem Au 2022, 2, 386−394